

## **AZD1152, a Selective Inhibitor of Aurora B Kinase, Inhibits Human Tumor Xenograft Growth by Inducing Apoptosis**

Robert W. Wilkinson,<sup>1</sup> Rajesh Odedra,<sup>1</sup> Simon P. Heaton,<sup>1</sup> Stephen R. Wedge,<sup>1</sup> Nicholas J. Keen,<sup>2</sup> Claire Crafter,<sup>1</sup> John R. Foster,<sup>1</sup> Madeleine C. Brady,<sup>1</sup> Alison Bigley,<sup>1</sup> Elaine Brown,<sup>1</sup> Kate F. Byth,<sup>2</sup> Nigel C. Barrass,<sup>1</sup> Kirsten E. Mundt,<sup>1</sup> Kevin M. Foote,<sup>1</sup> Nicola M. Heron,<sup>1</sup> Frederic H. Jung,<sup>3</sup> Andrew A. Mortlock,<sup>1</sup> F. Thomas Boyle,<sup>1,†</sup> and Stephen Green<sup>1</sup>

**Abstract Purpose:** In the current study, we examined the *in vivo* effects of AZD1152, a novel and specific inhibitor of Aurora kinase activity (with selectivity for Aurora B).

**Experimental Design:** The pharmacodynamic effects and efficacy of AZD1152 were determined in a panel of human tumor xenograft models. AZD1152 was dosed via several parenteral (s.c. osmotic mini-pump, i.p., and i.v.) routes.

**Results:** AZD1152 potentially inhibited the growth of human colon, lung, and hematologic tumor xenografts (mean tumor growth inhibition range, 55% to  $\geq 100\%$ ;  $P < 0.05$ ) in immunodeficient mice. Detailed pharmacodynamic analysis in colorectal SW620 tumor-bearing athymic rats treated i.v. with AZD1152 revealed a temporal sequence of phenotypic events in tumors: transient suppression of histone H3 phosphorylation followed by accumulation of 4N DNA in cells (2.4-fold higher compared with controls) and then an increased proportion of polyploid cells (>4N DNA, 2.3-fold higher compared with controls). Histologic analysis showed aberrant cell division that was concurrent with an increase in apoptosis in AZD1152-treated tumors. Bone marrow analyses revealed transient myelosuppression with the drug that was fully reversible following cessation of AZD1152 treatment.

**Conclusions:** These data suggest that selective targeting of Aurora B kinase may be a promising therapeutic approach for the treatment of a range of malignancies. In addition to the suppression of histone H3 phosphorylation, determination of tumor cell polyploidy and apoptosis may be useful biomarkers for this class of therapeutic agent. AZD1152 is currently in phase I trials.

The Aurora kinases play a critical role in mitosis and have been suggested as promising targets for cancer therapy due to their frequent overexpression in a variety of tumors (1). Compared with more established inhibitors of cell division, such as the anti-tubulins (2), novel agents that target mitotic enzymes have the potential to provide similar efficacy but with fewer side effects. Mammalian cells possess three forms of Aurora kinase (Aurora A, Aurora B, and Aurora C) that exhibit different subcellular localizations and have distinct roles (3, 4). However, it is still unclear which Aurora kinase represents the best target for anticancer therapy. Interestingly, inhibitors that

target both Aurora A and Aurora B induce a failure in cell division and endoreduplication rather than a G<sub>2</sub>-M arrest, effects that are indicative of Aurora B rather than Aurora A inhibition (5). Furthermore, it has been suggested that inhibition of Aurora B kinase overrides the effects of inhibition of Aurora A by abrogating the spindle checkpoint (6).

Several small-molecule inhibitors of Aurora kinases have been developed as anticancer agents, some of which have progressed to early clinical evaluation (7). ZM447439 (5), Hesperadin (8), and VX-680 (MK-0457; ref. 9) were the first to be described and have similar potency versus Aurora A, Aurora B, and Aurora C (reviewed in ref. 7). VX-680 also has activity versus Flt-3 and the imatinib-resistant T3511 Bcr-Abl mutant kinase (10). More recently, PHA-680632, a more potent inhibitor of Aurora A (IC<sub>50</sub>, 27 nmol/L) than Aurora B or Aurora C (IC<sub>50</sub>, 135 and 120 nmol/L, respectively), has been described, although the phenotypic effects induced in tumor cells by this compound (i.e., decreased phosphorylation of histone H3 on Ser<sup>10</sup> and polyploidy) are consistent with inhibition of Aurora B (11).

AZD1152 is a dihydrogen phosphate prodrug of a pyrazoloquinazoline Aurora kinase inhibitor [AZD1152-hydroxyquinazoline pyrazol anilide (HQPA)] and is converted rapidly to the active AZD1152-HQPA in plasma (12). AZD1152-HQPA is a highly potent and selective inhibitor of Aurora B

**Authors' Affiliations:** <sup>1</sup>AstraZeneca Pharmaceuticals, Macclesfield, Cheshire, United Kingdom; <sup>2</sup>Cancer and Infection Discovery, AstraZeneca Pharmaceuticals LP, Waltham, Massachusetts; and <sup>3</sup>AstraZeneca, Centre de Recherches, Reims, France Received 12/15/06; revised 2/21/07; accepted 3/5/07.

The costs of publication of this article were defrayed in part by the payment of page charges. This article must therefore be hereby marked *advertisement* in accordance with 18 U.S.C. Section 1734 solely to indicate this fact.

<sup>†</sup>Deceased.

**Note:** This work is presented in memory of Tom Boyle.

**Requests for reprints:** Robert W. Wilkinson, AstraZeneca Pharmaceuticals, Alderley Park, Macclesfield, Cheshire SK10 4TG, United Kingdom. Phone: 44-1625-516661; E-mail: robert.wilkinson@astrazeneca.com.

©2007 American Association for Cancer Research.

doi:10.1158/1078-0432.CCR-06-2979

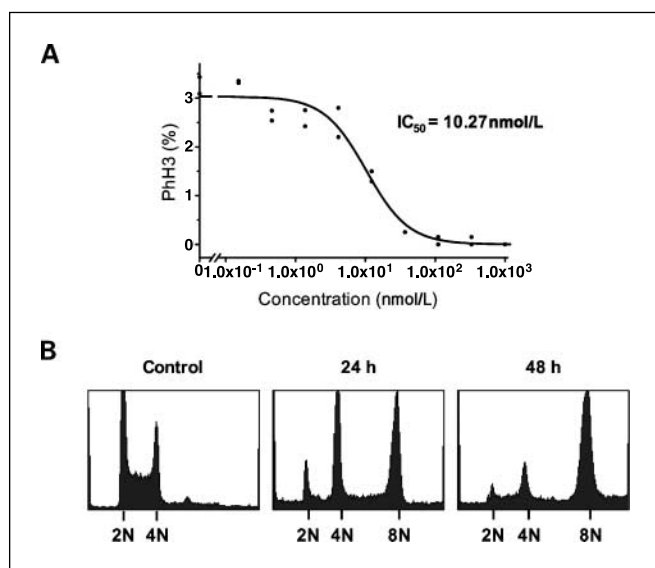


**Fig. 1.** AZD1152-HQPA inhibits histone H3 Ser<sup>10</sup> phosphorylation and induces polyploidy *in vitro*. *A*, a typical dose-response curve showing inhibition of histone H3 phosphorylation in SW620 cells following 48-h exposure to AZD1152-HQPA. The cells were analyzed on an Array Scan II. Data are representative of at least six separate experiments. *B*, flow cytometric DNA content histograms of SW620 cells exposed to 300 nmol/L AZD1152-HQPA for 0, 24, and 48 h, showing that cells fail to divide in the presence of AZD1152-HQPA and become polyloid.

( $K_i$ , 0.36 nmol/L) compared with Aurora A ( $K_i$ , 1,369 nmol/L) and has a high specificity versus a panel of 50 other kinases (13).<sup>4</sup> Consistent with inhibition of Aurora B kinase, addition of AZD1152-HQPA to tumor cells *in vitro* induces chromosome misalignment, prevents cell division, and consequently reduces cell viability and induces apoptosis (13).<sup>4</sup> The aim of the present study was to investigate the effects of AZD1152 administration in a panel of human tumor models *in vivo*. We show that AZD1152 (10-150 mg/kg/d, administered by s.c. osmotic mini-pump infusion over 48 h) induced time-dependent pharmacodynamic changes in tumors that were consistent with inhibition of Aurora B kinase *in vivo*, which led to significant inhibition of tumor xenograft growth. These data show that AZD1152 has the potential for activity against multiple tumor types and support investigation of this novel agent in cancer patients.

### Materials and Methods

**Reagents.** AZD1152-HQPA and its prodrug AZD1152 were both synthesized by AstraZeneca Pharmaceuticals (12).

**Cell lines.** The human colorectal (SW620, Colo205, and HCT116), lung (A549 and Calu-6), and leukemia (HL-60) tumor cell lines were obtained from the American Type Culture Collection. Cells were maintained *in vitro* using L-15 (SW620) or RPMI 1640 (Colo205, HCT116, A549, Calu-6, and HL-60) culture medium (all media were from Sigma), supplemented with 10% heat-inactivated FCS (Life Technologies) and 1% glutamine (Sigma; except SW620). All cell cultures were maintained in 5% CO<sub>2</sub> at 37°C in a humidified incubator, with the exception of SW620, which were grown in the absence of CO<sub>2</sub>.

<sup>4</sup> Submitted for publication.

**In vitro studies.** Phospho-histone H3 (PhH3) suppression was determined by high-content image analysis screening. SW620 cells, seeded in 96-well plates, were incubated with AZD1152-HQPA for 24 h before being fixed in 3.7% formaldehyde for 30 min. Cells were then washed with PBS, permeabilized with 0.5% Triton X-100 (Sigma), and stained with rabbit anti-PhH3 (Ser<sup>10</sup>) antibodies (1:100; Upstate Cell

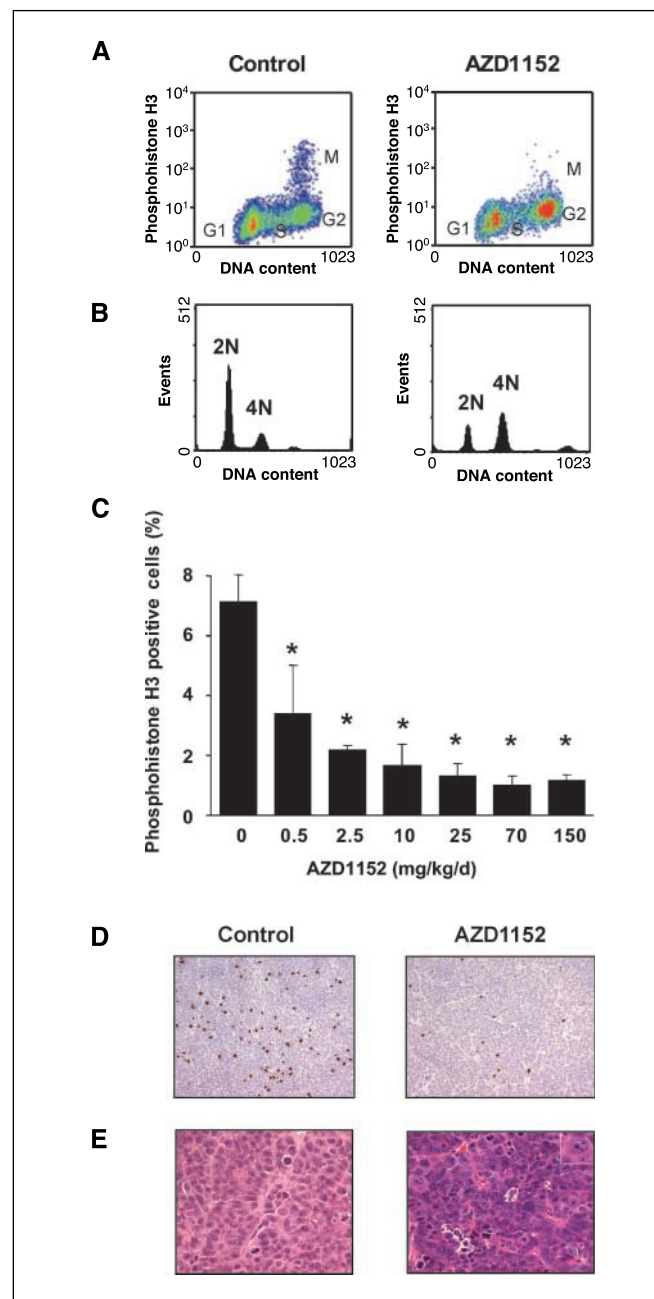


**Fig. 2.** AZD1152 blocks Aurora B activity in SW620 xenografts. Male nude mice were implanted subcutaneously with SW620 tumors. When tumors became palpable, animals ( $n = 4$  per group) were dosed with either AZD1152 (0.5-150 mg/kg/d) or vehicle as a constant infusion for 48 h using a s.c. mini-pump. Following treatment, tumors were excised and analyzed for pharmacodynamic effects. Flow cytometric analysis of disaggregated tumors from animals treated with AZD1152 (70 mg/kg/d) or vehicle showing changes in PhH3 (*A*) and DNA content (*B*). Dose-response curve showing percentage PhH3-positive cells in SW620 tumors analyzed by flow cytometry. Columns, PhH3-positive cells (%); bars, SE; \*,  $P < 0.05$ , (*C*). Representative sections of tumors treated with AZD1152 (70 mg/kg/d) or vehicle immunostained for PhH3 Ser<sup>10</sup> (*D*) and H&E (*E*). Inset denotes polypliodic cell.

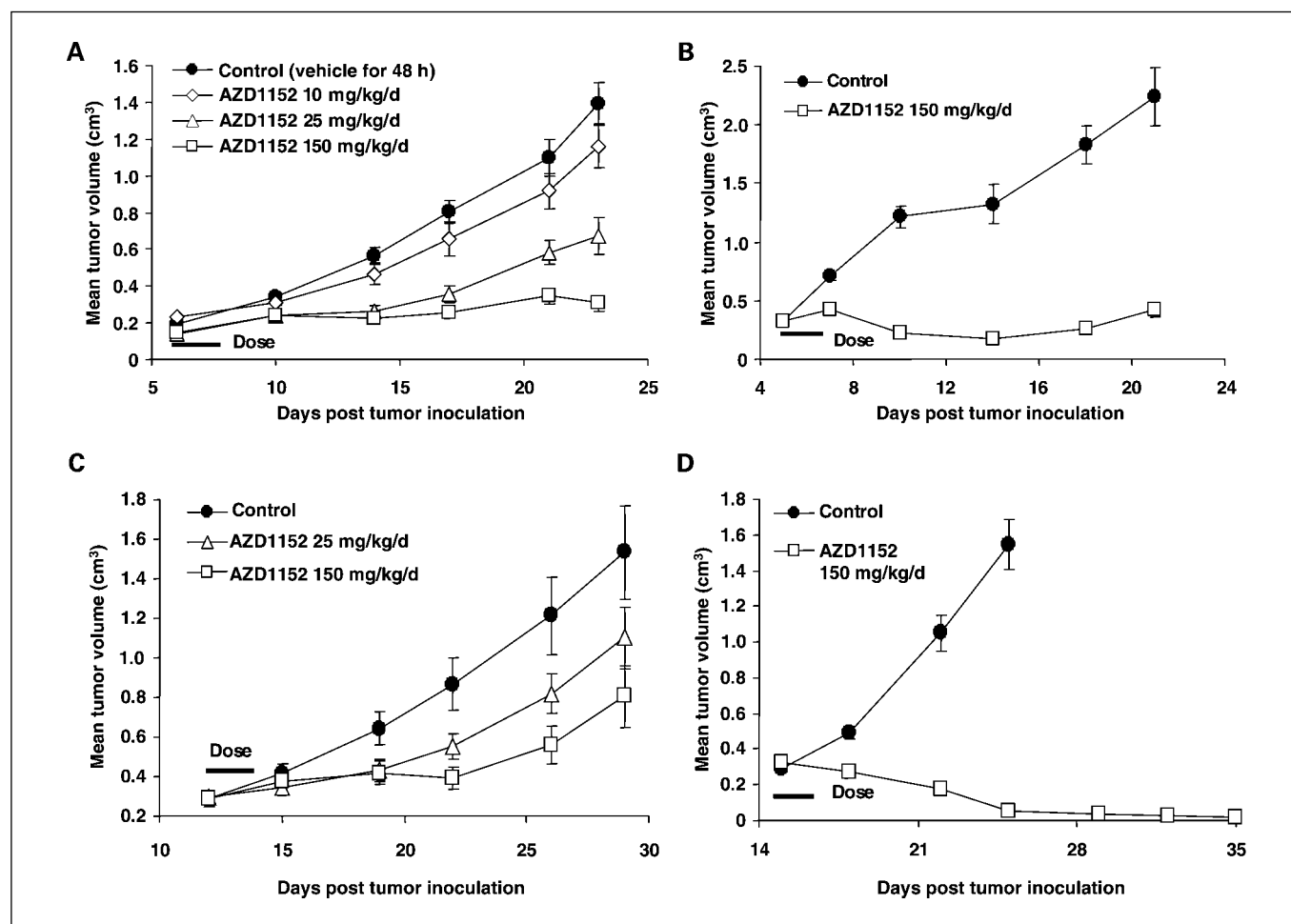


**Fig. 3.** AZD1152 inhibits growth in a panel of human tumor xenografts. Male nude mice bearing established SW620 (A), Colo205 (B), A549 (C), and HL-60 (D) human tumor xenografts were dosed s.c. at a constant infusion via an osmotic mini-pump for 48 h with either vehicle or AZD1152 (10-150 mg/kg/d). Mean tumor volume ( $\text{cm}^3$ ) of 8 to 10 mice; vertical bars, SE; horizontal bars, duration of dosing.

Signaling Solutions) for 1 h at room temperature. After washing with PBS, cells were incubated with Alexa Fluor 488 goat anti-rabbit antibodies (1:200; Molecular Probes) and Hoechst stain (1:10,000; Molecular Probes) for 1 h at room temperature. Cellular levels of PhH3 were analyzed on the Array Scan II (Cellomics) using the Target Activation algorithm (Cellomics) to calculate the percentage of PhH3-positive cells. Individual  $\text{IC}_{50}$  values were calculated in Origin (version 7.5; OriginLab) and the data were summarized using the geometric mean (i.e., the average of the logarithmic values converted back to a base 10 number).

**In vivo studies.** Male Swiss nude (*nu/nu* genotype; AstraZeneca), SCID-bg mice (CB17/1cr.Cg.Prkdc<sup>SCID</sup>Lyst<sup>bg</sup>/Crl; Charles River), or nude rats (Nude:Hsd Han:RNU-rnu; AstraZeneca) were housed in negative pressure isolators (PFI Systems Ltd.) or in an individually ventilated cage system (Tecniplast Ltd.). Experiments were conducted on 8- to 12-week-old animals in full accordance with the United Kingdom Home Office Animal (Scientific Procedures) Act 1986. Human tumor xenografts were established by s.c. injecting 100 to 200  $\mu\text{L}$  tumor cells (between  $1 \times 10^6$  and  $1 \times 10^7$  cells mixed 50:50 with Matrigel; Becton Dickinson) on the flank. Animals were randomized into treatment groups ( $n = 8-11$  per group) when tumors reached a defined palpable size (0.2-0.3  $\text{cm}^3$  and 0.5-1  $\text{cm}^3$  for mice and rats, respectively). AZD1152 was prepared in Tris buffer (pH 9) and administered either as a bolus injection (i.v. or i.p.) or as a continuous 48-h infusion via s.c. implanted osmotic mini-pumps (two 24-h pumps implanted sequentially; model 2001D, Durect Corp.) in accordance

with the manufacturer's instructions. Tumors were measured up to three times weekly with calipers, tumor volumes were calculated, and the data were plotted using the geometric mean for each group versus time. Tumor volume and tumor growth inhibition were calculated as described previously (14). Statistical analysis of any change in tumor volume was carried out using a Student's one-tailed *t* test (*P* value of  $<0.05$  was considered to be statistically significant).

For pharmacodynamic time course studies, nude rats bearing established SW620 tumor xenografts received vehicle or AZD1152 (25 mg/kg/d) as a daily i.v. bolus dose for 4 consecutive days (days 1-4). At multiple time points after dosing (days 0, 5, 9, 12, 16, and 19), two subgroups ( $n = 3$  per group) of either vehicle- or AZD1152-treated animals were humanely killed and tumor and normal proliferating tissues (including bone marrow) were excised and assessed for pharmacodynamic effects using flow cytometric, histologic, or immunohistochemical analysis.

**Flow cytometry.** For *in vitro* studies, SW620 cells in logarithmic growth phase were exposed to 50 nmol/L AZD1152-HQPA for 24 or 48 h and then fixed in 70% ethanol at  $-20^\circ\text{C}$  overnight. Cells were rehydrated in PBS and resuspended in PBS containing 100  $\mu\text{g}/\text{mL}$  RNase (Sigma) and 10  $\mu\text{g}/\text{mL}$  propidium iodide (Sigma), and cellular DNA content was analyzed on a FACSCalibur flow cytometer (Becton Dickinson). A total of 15,000 cells were counted and phases of the cell cycle were assessed using CellQuest software (Becton Dickinson). For tumor samples, cell suspensions were prepared from the snap-frozen

tumors using an automated tissue disaggregation system (Medimachine, BD Biosystems) and fixed in 80% ethanol for a minimum of 24 h. Once fixed, disaggregated tumors were prepared for DNA content and PhH3 analysis by flow cytometry following a previously described immunofluorescent staining protocol (15) using propidium iodide and the same commercially available antibodies [PhH3, rabbit polyclonal IgG (Upstate Biotechnology) and fluorescein-conjugated goat anti-rabbit IgG (Jackson ImmunoResearch)].

**Histology and immunohistochemistry.** For histologic analyses, tumors and femurs were fixed in formalin for 24 to 48 h and then processed to paraffin wax blocks. Femurs were decalcified using 10% formic acid before being processed to paraffin blocks. Tissue sections (3-4  $\mu$ m thick) were stained with H&E. For immunohistochemical studies, sections were stained with rabbit polyclonal antibodies directed against either PhH3 or cleaved caspase-3 (Cell Signaling Technology) followed by a one-step horseradish peroxidase-labeled polymer method (Envision; DakoCytomation). Sections were counterstained with Carazzi's hematoxylin. Analysis of immunostaining in tumor sections was done on a Zeiss KS400 image analysis system (version 3; Imaging Associates Ltd.) linked to a Leica DMRB microscope. The KS400 is a color space/morphologic image analyzer for which thresholds of hue, luminosity, and saturation were set relative to the brown chromagen used for the immunolocalization of cleaved caspase-3. Area of cleaved caspase-3 immunostaining was quantified using an in-house macro to calculate the average percentage area of brown staining per area of field of vision (six fields per evaluable tumor section;  $\times 20$  magnification).

## Results

**AZD1152-HQPA inhibits Aurora B kinase activity and prevents cell division.** AZD1152-HQPA has been shown previously to be a highly potent inhibitor of Aurora kinase enzyme activity *in vitro*, with selectivity for Aurora B kinase (Aurora B-INCENP  $K_i$  of 0.36 nmol/L) versus Aurora A ( $K_i$  of 1,369 nmol/L) and Aurora C (Aurora C-INCENP  $K_i$  of 17 nmol/L; ref. 13).<sup>4</sup> Consistent with Aurora B kinase inhibition, exposure of human SW620 colorectal tumor cells to AZD1152-HQPA resulted in a

dose-dependent inhibition of histone H3 phosphorylation on Ser<sup>10</sup> (Fig. 1A) that led to an increase in polyploidy following a 48-h exposure (Fig. 1B).

**AZD1152 administration leads to inhibition of Aurora B kinase activity in vivo.** Pharmacokinetic studies confirmed that AZD1152 was rapidly converted to the active drug AZD1152-HQPA in mouse and rat following systemic administration (data not shown). To determine whether AZD1152 administration leads to inhibition of Aurora B kinase activity in human tumor xenografts, we first examined PhH3 and DNA ploidy in SW620 colon tumors (established in nude mice) following s.c. infusion (by osmotic mini-pump) of AZD1152 (0.5-150 mg/kg) or vehicle over 48 h. Flow cytometric analysis of disaggregated tumor xenografts showed that the proportion of PhH3-positive cells within the G<sub>2</sub>-M phase of the cell cycle was markedly reduced in AZD1152-treated animals compared with those receiving vehicle (AZD1152 at 70 mg/kg/d; Fig. 2A). Significant suppression of PhH3 was evident following 48-h administration of AZD1152, at doses as low as 0.5 mg/kg/d (52% inhibition). This inhibition increased further with 2.5 mg/kg/d AZD1152 (to 69%), whereas doses of 10 to 150 mg/kg/d resulted in between 77% and 86% inhibition (Fig. 2C).

Flow cytometric analysis of the DNA content (2N, 4N, and >4N) of tumors indicated an increased proportion of cells with a 4N and >4N DNA content from animals that received AZD1152 (AZD1152 at 70 mg/kg/d; Fig. 2B). The proportion of 2N and 4N DNA content was 58% and 24%, respectively, in tumors from vehicle-treated mice, whereas in tumors retrieved from mice receiving AZD1152 (70 mg/kg/d) treatment, the proportions were reversed, with 35% of cells showing 2N and 56% of cells showing 4N DNA content. This accumulation of cells with 4N DNA content is consistent with failed cytokinesis and continued cell cycle progression following inhibition of Aurora kinase activity. These findings were supported by histologic data, which showed a reduction of PhH3 and an increase in large multinucleated cells in AZD1152-treated

**Table 1.** *In vivo* activity of AZD1152 against a range of human tumor xenograft models

Tumor model	Tumor origin	Dose (mg/kg/d)	Route (duration)	Inhibition of tumor volume (%)	
				Maximum	End of study
SW620	Human colon	150	S.c. mini-pump (48 h, days 7-9)	87* (day 23)	87* (day 23)
		25	S.c. mini-pump (48 h, days 7-9)	65 <sup>†</sup> (day 14)	49 <sup>†</sup> (day 23)
		10	S.c. mini-pump (48 h, days 7-9)	55 <sup>‡</sup> (day 10)	28 <sup>‡</sup> (day 23)
		25	I.p. bolus daily (4 d, days 6-9)	65 <sup>†</sup> (day 13)	54* (day 24)
		25	I.v. bolus daily (3 d, days 6-8)	91* (day 13)	47 <sup>†</sup> (day 24)
Colo205	Human colon	150	S.c. mini-pump (48 h, days 5-7)	>100* (day 18)	94* (day 21)
HCT116	Human colon	150	S.c. mini-pump (48 h, days 11-13)	93* (day 18)	74* (day 25)
A549	Human lung	150	S.c. mini-pump (48 h, days 13-15)	79 <sup>†</sup> (day 26)	69 <sup>†</sup> (day 29)
		25	S.c. mini-pump (48 h, days 13-15)	74 <sup>‡</sup> (day 15)	36 <sup>‡</sup> (day 29)
Calu-6	Human lung	150	S.c. mini-pump (48 h, days 20-22)	67 <sup>†</sup> (day 29)	55* (day 41)
HL-60 <sup>§</sup>	Human leukemia	150	S.c. mini-pump (48 h, days 16-18)	>100* (day 18)	>100* (day 35)

NOTE: Human tumor xenografts were established in the flank of male Swiss athymic mice (8-12 wks of age). Mice were randomized into treatment groups when tumors reached a mean volume of 0.2 to 0.5 cm<sup>3</sup> and then treated with a continuous infusion of AZD1152 or vehicle (0.3 mol/L Tris buffer) via a s.c. implanted mini-pump or as a once-daily i.p. or i.v. bolus. Percentage tumor growth inhibition was calculated as the difference between the change in control and AZD1152-treated tumor volumes during and following the treatment period. Statistical significance was calculated using a one-tailed *t* test. *P* value of <0.05 was considered to be statistically significant.

\**P* < 0.0005.

<sup>†</sup>*P* < 0.005.

<sup>‡</sup>*P* < 0.05.

<sup>§</sup>No palpable or measurable tumors in 8 of 11 animals following treatment with AZD1152.

tumors when compared with vehicle controls (AZD1152 at 70 mg/kg/d; Fig. 2D and E, respectively). These data indicate that the mechanism of action of AZD1152 *in vivo* recapitulates that observed with AZD1152-HQPA *in vitro* (13).<sup>4</sup>

**AZD1152 inhibits the growth of human tumor xenografts.** AZD1152 (10-150 mg/kg/d; s.c. mini-pump infusion over 48 h) exerted potent, dose-dependent inhibition of growth in s.c. implanted human colorectal (SW620, HCT116, and Colo205), lung (A549 and Calu-6), and hematologic (HL-60) tumor xenografts in immunodeficient mice. The inhibition of tumor growth in individual models ranged from 55% to  $\geq 100\%$  (all  $P < 0.05$ ; Fig. 3A-D; Table 1). HL-60 tumor xenografts were the most responsive to AZD1152, with complete tumor regression (i.e., no measurable tumors) at the end of the study in 8 of 11 animals (Fig. 3D). Significant antitumor activity was also observed when AZD1152 was dosed episodically to mice using other parenteral routes (i.e., i.v. or i.p. bolus injections). For example, three consecutive daily bolus i.v. injections of AZD1152 (25 mg/kg/d) in SW620-bearing mice led to a maximal tumor volume inhibition of 91% ( $P < 0.0005$ ; Table 1).

**Temporal pharmacodynamic analysis of AZD1152-sensitive tumors.** To analyze the molecular and cellular events that lead to tumor growth inhibition in xenograft models, we established an episodic AZD1152 dosing schedule (25 mg/kg i.v. bolus once daily from days 1 to 4) in nude rats bearing established SW620 tumor xenografts. Treatment with AZD1152 resulted in significant tumor growth inhibition that was maximal (93%) at 8 days after the final dose (Fig. 4A). Flow cytometry revealed that PhH3 was suppressed by  $\sim 40\%$  to 50% during the dosing period (days 1-4), with levels returning to baseline by day 9. There was also a transient increase in the proportion of both 4N (30% in vehicle versus 60% in AZD1152 treated) and polyploid ( $\geq 8N$ ; 23% in vehicle versus 67% in AZD1152 treated) tumor cells, which peaked between days 1 to 5 (Fig. 4B).

Histologic assessment of tumor cells obtained from vehicle-treated animals on day 5 (24 h after the final dose) displayed relative uniformity in cell size and morphology (Fig. 5A). In contrast, tumors from AZD1152-treated rats exhibited a high degree of pleomorphism and displayed morphologic characteristics that were indicative of apoptosis. Consistent with a failure of cell division, tumor cells from AZD1152-treated rats were larger than those from control animals receiving vehicle alone. Furthermore, even larger multinucleated tumor cells were evident by day 9 (5 days after the final dose of AZD1152). Staining and quantification of tumor samples for the apoptotic marker cleaved caspase-3 showed elevated levels following AZD1152 treatment compared with controls, particularly in the markedly enlarged cells observed at day 9 (Fig. 5B and D). This suggests that apoptosis is the final fate of cells exposed to AZD1152-HQPA during cell division (Fig. 5E).

Bone marrow tissue was used to study the effects of AZD1152 administration on a normal rapidly cycling cellular compartment. The bone marrow micrographs from vehicle-treated rats (day 5) were densely populated with hematopoietic cells and exhibited a normal histologic appearance (Fig. 5C). In comparison, the bone marrow micrographs from rats receiving AZD1152 and sampled on day 5 displayed signs of atrophy, with a marked reduction in total cellular content (Fig. 5C). However, the bone marrow had recovered markedly by day 9

(5 days after the last dose of AZD1152) and was repopulated with hematologic cells of a histologically normal appearance (Fig. 5C). Flow cytometric analysis of bone marrow and peripheral whole blood cells from the same animal groups also indicated transient AZD1152-induced myelosuppression, with neutrophils being the most affected leukocyte population (data not shown). AZD1152 was otherwise well tolerated at doses where antitumor efficacy was observed; compared with vehicle-treated animals, AZD1152-treated athymic rats had a mean maximal body weight loss of 5%, 24 h following 4 days of treatment (25 mg/kg/d i.v. daily for four consecutive days), and regained body weight thereafter.

## Discussion

AZD1152, a specific Aurora kinase inhibitor with selectivity for Aurora B kinase, is a dihydrogen phosphate prodrug that is highly soluble in simple pH-adjusted aqueous vehicles, making it suitable for parenteral dosing. In mouse and rat, AZD1152 undergoes rapid systemic conversion to the active drug AZD1152-HQPA, which has pharmacokinetic properties that cause dose-dependent plasma exposure (12).

These data confirmed that AZD1152 was converted to the active drug AZD1152-HQPA *in vivo* and elicited pharmacodynamic effects consistent with inhibition of Aurora B kinase. We have shown that administering AZD1152 to animals

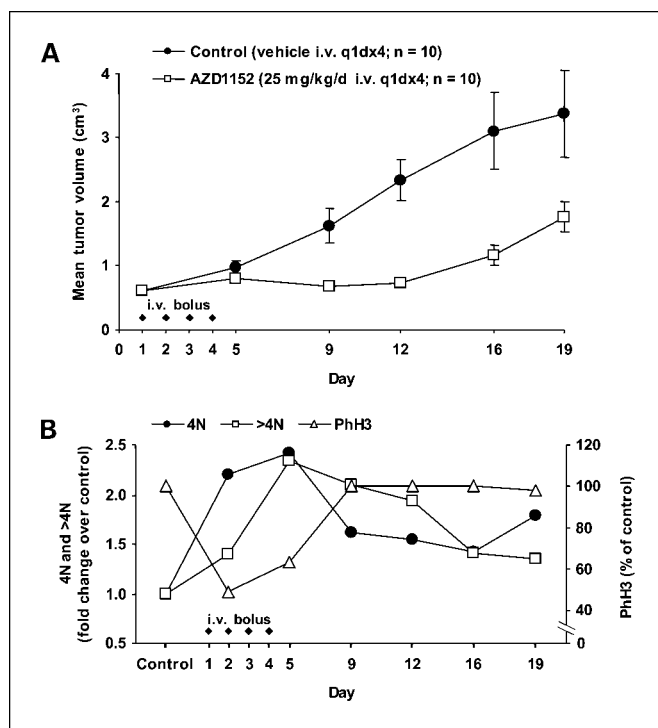
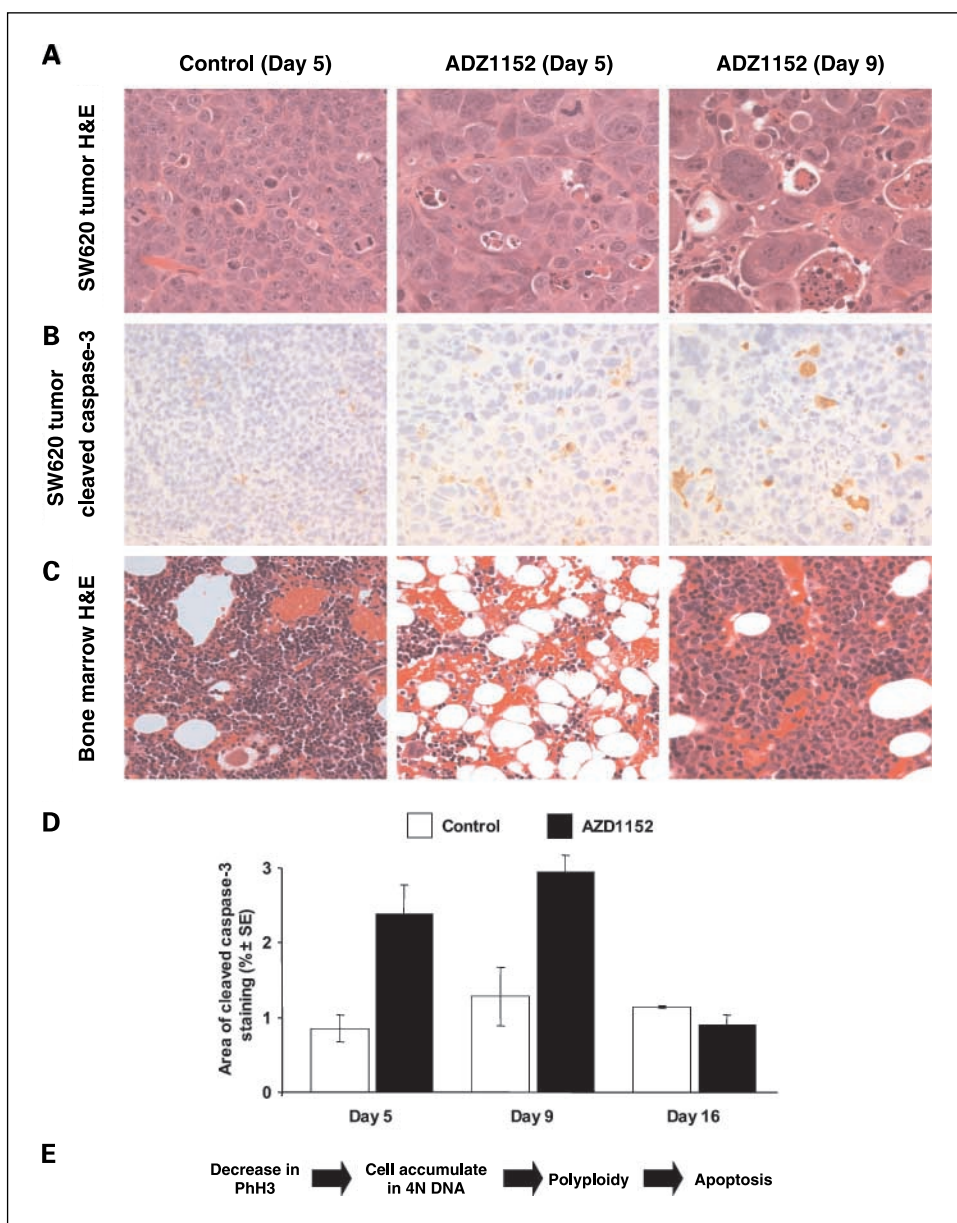


**Fig. 4.** Chronological characterization of AZD1152-induced antitumor responses. Male nude rats ( $n = 28$  per group) bearing established SW620 tumor xenografts were dosed daily (once daily) with either vehicle or AZD1152 (i.v. bolus, 25 mg/kg) for 4 consecutive days. Subgroups of rats ( $n = 3$  per group per time point) were removed during the experiment (days 0, 5, 9, 12, 16, and 19 from start of dosing) and tumor tissue was analyzed for pharmacodynamic effects using flow cytometry as described in Materials and Methods. **A**, tumor growth inhibition response. Mean tumor volume ( $\text{cm}^3$ ;  $n = 10$ ); bars, SE. **B**, flow cytometric analysis of disaggregated tumors showing PhH3 (expressed as percentage of control) and 4N DNA or polyploid ( $>4N$ ) DNA content (expressed as fold increase over control) changes.

**Fig. 5.** AZD1152 treatment leads to phenotypic changes in tumor and hematologic tissue. Excised tissue derived from the antitumor study described in Fig. 4 also underwent histologic analyses (A-C). Representative sections of tumor (A and B) and bone marrow (C) taken on days 1 and 4 after the final dose of AZD1152 are shown (middle and right, respectively) and compared with corresponding sections from vehicle-treated animals taken on day 1 (left). Sections were stained with H&E (A and C) and immunoreactivity for cleaved caspase-3 (B). Magnification,  $\times 40$ . D, quantitative analysis by scanning microscopy of cleaved caspase-3-immunostained tumors. Columns, mean of one experiment ( $n = 3$  animals per group per time point, one tumor section per animal, six fields per tumor); bars, SE. E, the proposed sequence of events occurring in AZD1152-treated tumor tissue.



bearing human tumor xenografts leads to an inhibition of histone H3 phosphorylation followed by a failure of tumor cell division, endoreduplication, and an induction of tumor cell death by apoptosis. Moreover, these findings are consistent with the observed effects of AZD1152-HQPA *in vitro* (13)<sup>4</sup> and are distinct from the phenotype associated with antimetabolic/anti-tubulin agents, such as paclitaxel (i.e., where cells usually arrest in mitosis; refs. 2, 16).

Parenteral administration of AZD1152 resulted in profound antitumor effects in each of the colorectal, lung, and acute myeloid leukemia human tumor xenograft models examined. This antitumor response persisted for a considerable time after the end of dosing. Furthermore, in the HL-60 acute myeloid leukemia model, durable regressions were observed over a 20-day period, with no palpable tumors observed in 8 of 11 animals. The responsiveness of HL-60 xenografts to Aurora kinase inhibitors has also been reported in two independent

studies using the mixed Aurora (Aurora A/Aurora B) inhibitors VX-680 and PHA-680632 (9, 11): VX-680 (75 mg/kg administered twice daily by i.p. injection for 13 days) inhibited HL-60 tumor growth by 98% and PHA-680632 (45 mg/kg administered twice daily by i.v. injection for 5 days) inhibited growth by 85%. The effect of administering AZD1152 via different dosing schedules was investigated further in nude mice bearing colorectal tumor xenografts. Significant antitumor activity was observed in tumors following dosing of AZD1152 either at high doses for short durations (i.v. or i.p. bolus injections) or at lower doses for longer durations using s.c. osmotic minipumps. This suggests that examination of different clinical schedules may be warranted either as a monotherapy or in combination with existing therapeutic modalities.

Analyses of tissue from AZD1152-treated tumors showed a sequence of molecular/cellular events following the inhibition of Aurora B activity that was consistent with a failure of cell

division leading ultimately to apoptosis. Initial suppression of PhH3 was followed by a transient accumulation of 4N cells, with subsequent accumulation of polyploid cells. Histologic examination showed increased apoptosis in AZD1152-treated tumors compared with control, which reached a maximum over a time scale corresponding with the decline of polyploid cells observed by flow cytometry, and declined thereafter. These results support a mechanism by which induction of endoreduplication leads to polyploidy and eventual apoptosis. Previous studies investigating the effects of Aurora kinase inhibitors have proposed PhH3 as a surrogate marker of activity (9, 11). In the current study, PhH3 was found to be a sensitive and highly dynamic marker of Aurora kinase inhibition. The number of cells positive for PhH3 declined significantly after treatment across all AZD1152 concentrations tested and recovered rapidly after cessation of dosing. Interestingly, dose-dependent suppression of PhH3 occurred across a lower concentration range than dose-dependent inhibition of tumor growth. This difference may reflect the involvement of Aurora kinase substrates other than histone H3 in mediating effects on cytokinesis. Indeed, although PhH3 is widely used as a marker for Aurora kinase inhibition, its biological relevance to cytokinesis is not clear. Other putative Aurora B kinase substrates involved in cytokinesis include vimentin, GFAP, desmin, MgcRacGAP, and motorprotein MKlp1 (17–20). Considering all of the above, the dynamics of PhH3 suppression may be more predictive of therapeutic outcome when examined in conjunction with downstream phenotypic markers, such as tumor cell polyploidy and apoptosis.

There are several limitations with the currently available drugs that act by targeting mitosis. For example, agents that bind tubulin are associated with peripheral neuropathy (21). In this study, AZD1152 was well tolerated within the dose range required to elicit a potent and durable antitumor effect, with animals showing only transient loss of body weight. Bone marrow analyses revealed reversible myelosuppression in

AZD1152-treated animals, with full recovery occurring within a week of cessation of dosing. Analysis of peripheral blood cells also indicated a reduction in WBC counts (mainly neutropenia) followed by full recovery. These findings suggest that intermittent dosing schedules at appropriate intervals can be used to repeatedly target tumor cells while allowing bone marrow to recover. One reason may be the difference in proliferative rates during hematopoiesis, with bone marrow stem cells and progenitor cells having relatively low frequency of division, compared with late-stage differentiating neutrophils (22). This may explain the rapid reduction in absolute neutrophil counts that is followed by fast recovery of the bone marrow after withdrawal of AZD1152. Furthermore, normal cells may be less susceptible to the induction of polyploidy due to the presence of functional p53 (23).

In conclusion, these data show that inhibition of Aurora B activity *in vivo* has profound effects on tumor growth and that AZD1152 has the potential for efficacy in multiple tumor types. Moreover, the pharmacodynamic and efficacy results indicate that the major effects of AZD1152-HQPA on tumor cells *in vitro* are recapitulated with AZD1152 *in vivo*. In addition, simultaneous tracking of time-dependent changes in PhH3, polyploidy, and apoptosis provided an important and useful insight into how the antitumor effects of AZD1152 are mediated. This may ultimately lead to a strategy for monitoring the biological consequences of Aurora B kinase inhibition in the clinic. AZD1152 is currently undergoing phase I clinical evaluation as a treatment for cancer.

## Acknowledgments

We thank Sharon Barnett, Nicola Haupt, David Smith, Julie Humphreys, Keith Welsh, Darren Harrison, and Nigel Leake from the CDMG for technical assistance; Kerry Ratcliffe for histologic support; Julia Young, Joanne Wilson, and Mike Walker for pharmacokinetic support; Dereck Amakye and Andrew Hughes for translational science input; Chris Watson and Matthew Lewis of Mudskipper Bioscience for editorial support; and AZD1152 chemistry team for kindly providing compounds.

## References

- Andrews PD. Aurora kinases: shining lights on the therapeutic horizon? *Oncogene* 2005;24:5005–15.
- Wood KW, Cornwell WD, Jackson JR. Past and future of the mitotic spindle as an oncology target. *Curr Opin Pharmacol* 2001;1:370–7.
- Carmena M, Earnshaw WC. The cellular geography of aurora kinases. *Nat Rev Mol Cell Biol* 2003;4:842–54.
- Ducat D, Zheng Y. Aurora kinases in spindle assembly and chromosome segregation. *Exp Cell Res* 2004;301:60–7.
- Ditchfield C, Johnson VL, Tighe A, et al. Aurora B couples chromosome alignment with anaphase by targeting BubR1, Mad2, and Cenp-E to kinetochores. *J Cell Biol* 2003;161:267–80.
- Yang H, Burke T, Dempsey J, et al. Mitotic requirement for aurora A kinase is bypassed in the absence of aurora B kinase. *FEBS Lett* 2005;579:3385–91.
- Keen N, Taylor S. Aurora-kinase inhibitors as anticancer agents. *Nat Rev Cancer* 2004;4:927–36.
- Hauf S, Cole RW, LaTerra S, et al. The small molecule Hesperadin reveals a role for Aurora B in correcting kinetochore-microtubule attachment and in maintaining the spindle assembly checkpoint. *J Cell Biol* 2003;161:281–94.
- Harrington EA, Bebbington D, Moore J, et al. VX-680, a potent and selective small-molecule inhibitor of the Aurora kinases, suppresses tumor growth *in vivo*. *Nat Med* 2004;10:262–7.
- Young MA, Shah NP, Chao LH, et al. Structure of the kinase domain of an imatinib-resistant Abl mutant in complex with the Aurora kinase inhibitor VX-680. *Cancer Res* 2006;66:1007–14.
- Soncini C, Carpinelli P, Gianellini L, et al. PHA-680632, a novel Aurora kinase inhibitor with potent antitumoral activity. *Clin Cancer Res* 2006;12:4080–9.
- Mortlock AA, Foote KM, Heron NM, et al. Discovery, synthesis and *in vivo* activity of a new class of pyrazoloquinazolines as selective inhibitors of aurora B kinase. *J Med Chem* 2007;50:2213–24.
- Keen N, Brown E, Crafter C, et al. Biological characterization of AZD1152, a highly potent and selective inhibitor of aurora kinase activity. *Clin Cancer Res* 2005;11:B220.
- Wedge SR, Kendrew J, Hennequin LF, et al. AZD2171: a highly potent, orally bioavailable, vascular endothelial growth factor receptor-2 tyrosine kinase inhibitor for the treatment of cancer. *Cancer Res* 2005;65:4389–400.
- Widrow RJ, Laird CD. Enrichment for submitotic cell populations using flow cytometry. *Cytometry* 2000;39:126–30.
- Chen JG, Horwitz SB. Differential mitotic responses to microtubule-stabilizing and -destabilizing drugs. *Cancer Res* 2002;62:1935–8.
- Goto H, Yasui Y, Kawajiri A, et al. Aurora-B regulates the cleavage furrow-specific vimentin phosphorylation in the cytokinetic process. *J Biol Chem* 2003;278:8526–30.
- Kawajiri A, Yasui Y, Goto H, et al. Functional significance of the specific sites phosphorylated in desmin at cleavage furrow: Aurora-B may phosphorylate and regulate type III intermediate filaments during cytokinesis coordinately with Rho-kinase. *Mol Biol Cell* 2003;14:1489–500.
- Minoshima Y, Kawashima T, Hirose K, et al. Phosphorylation by aurora B converts MgcRacGAP to a Rho-GAP during cytokinesis. *Dev Cell* 2003;4:549–60.
- Neef R, Klein UR, Kopajtic R, Barr FA. Cooperation between mitotic kinesins controls the late stages of cytokinesis. *Curr Biol* 2006;16:301–7.
- Scuteri A, Nicolini G, Miloso M, et al. Paclitaxel toxicity in post-mitotic dorsal root ganglion (DRG) cells. *Anticancer Res* 2006;26:1065–70.
- Kondo M, Wagers AJ, Manz MG, et al. Biology of hematopoietic stem cells and progenitors: implications for clinical application. *Annu Rev Immunol* 2003;21:759–806.
- Margolis RL. Tetraploidy and tumor development. *Cancer Cell* 2005;8:353–4.

# Clinical Cancer Research

## AZD1152, a Selective Inhibitor of Aurora B Kinase, Inhibits Human Tumor Xenograft Growth by Inducing Apoptosis

Robert W. Wilkinson, Rajesh Odedra, Simon P. Heaton, et al.

*Clin Cancer Res* 2007;13:3682-3688.

**Updated version** Access the most recent version of this article at:  
<http://clincancerres.aacrjournals.org/content/13/12/3682>

**Cited articles** This article cites 23 articles, 9 of which you can access for free at:  
<http://clincancerres.aacrjournals.org/content/13/12/3682.full#ref-list-1>

**Citing articles** This article has been cited by 59 HighWire-hosted articles. Access the articles at:  
<http://clincancerres.aacrjournals.org/content/13/12/3682.full#related-urls>

**E-mail alerts** [Sign up to receive free email-alerts](#) related to this article or journal.

**Reprints and Subscriptions** To order reprints of this article or to subscribe to the journal, contact the AACR Publications Department at [pubs@aacr.org](mailto:pubs@aacr.org).

**Permissions** To request permission to re-use all or part of this article, use this link  
<http://clincancerres.aacrjournals.org/content/13/12/3682>.  
Click on "Request Permissions" which will take you to the Copyright Clearance Center's (CCC) Rightslink site.